



Effects of Amine Fluoride Cleaning Chemistry on Metallic Aluminum IC Films

II. Determining Causal Chemistry of OCPs by a Time-Dependent Free Energy Relationship

Melvin Keith Carter²

DuPont Electronics Technologies, EKC Technology, Hayward, California 94545, USA

A mathematical expression has been developed describing the change in thermodynamic free energy for a chemical system as a function of time to aid the interpretation of experimental time-dependent energy curves, such as the open circuit potential (OCP) plots, generated in corrosion studies. Accurate results of chemical potentials and reaction rates, one pair of constants for each causal chemical reaction, were found. Reaction rate constants were determined for OCPs of $\text{Fe}(\text{CN})_6^{4-} + 1/2\text{I}_2 \rightarrow \text{Fe}(\text{CN})_6^{3-} + \text{I}^-$ at room temperature of $\omega_1 = 0.011 \pm 0.002/\text{s}$, for oxidation of $\text{Fe}(\text{CN})_6^{4-}$ to $\text{Fe}(\text{CN})_6^{3-}$ and $\omega_2 = 0.108 + 0.003/\text{s}$ for reduction of I_2 to I^- , and the known half-cell potentials were reproduced. Experimental aluminum dissolution OCP data was fit using regression analysis describing a four to ten chemical reaction model. The formalism was useful in describing results of OCP plots of integrated circuits (IC) interconnect metals, cleaned by fluoride-based silicon wafer remover formulas, in terms of identifying the causal corrosion chemistry.

© 2004 The Electrochemical Society. [DOI: 10.1149/1.1836152] All rights reserved.

Manuscript submitted March 30, 2004; revised manuscript received June 3, 2004. Available electronically December 7, 2004.

Integrated circuits (ICs) with submicrometer aluminum interconnects are commonly cleaned using liquid chemical products designed specifically to remove postplasma etch residues with minimal corrosion damage of the metal surfaces. These products are typically water/solvent formulations, containing active fluoride additives and pH regulators, designed to clean high-feature density silicon wafers. In Part I, Experimental Measurements and Chemical Modeling,¹ it was shown that formula FA removed surface residues and passivation layers from aluminum-coated silicon wafer surfaces. A number of electrochemical experiments were conducted to illuminate the variables of the chemical cleaning process in an attempt to discover the chemical mechanism of aluminum dissolution (corrosion). A process model was established and an indicated chemical model was proposed consisting of a sequence of time-dependent reactions describing a multisloped open circuit electrochemical potential (OCP), with a corresponding current flow of 6×10^{-9} A, presented here as Fig. 4a. Ideally, detailed chemical analysis could be conducted to measure chemical concentration changes associated with each step of the OCP measurement, but such analyses are impractical at ultralow concentration levels. The purpose of this work is to develop a mathematical formalism to relate experimental OCP data curves to their underlying causal chemistries so that the desired chemical potential and reaction rate constant might be revealed for each contributing chemical reaction in a set of reactions.

Thermodynamics addresses energy changes associated with chemical reactions based on a definition of a system as being at rest ($\Delta F \approx 0$). The potential E° of an electric cell is given at that potential representing the final oxidation state of an element at a condition of rest so no current flows between the electrodes. In reality a small amount of current must flow to establish a working cell and to allow measurement of the cell potential. Thus, real systems are not exactly at equilibrium but approach equilibrium. It is precisely this gray area as systems approach equilibrium in which kinetics is also often described.

A kinetic system is a chemical organization in unidirectional motion² while a thermodynamic system is normally at or approaching equilibrium. Energy is conserved so a kinetic system can comply with the first law of thermodynamics. The term kinetics, however, implies that a system is not at rest and, therefore, not precisely in thermodynamic equilibrium (not in strict compliance with the second law of thermodynamics).³ Thus, there is an apparent chasm

between thermodynamic equilibrium and kinetic systems such that they may not be defined at precisely the same conditions.

Kinetic reaction rates are commonly expressed in terms of differential equations⁴ such as $dC_a/dt = -k_a C_a$ that describe the change in concentration with time near equilibrium as the rate k_a of the instantaneous change in the concentration of species a ignoring the other simultaneous changes that must be occurring. Changes in other components are tacitly ignored and are assumed to be small, or independent thereof, compared to the changes in a. It is apparent that real thermodynamic and kinetic systems approach equilibrium rather than operating at equilibrium. Nonetheless, kinetic modeling methods have produced considerable useful information, although often approximate. A relation has been expressed⁵ between reaction rates and an exponential function of free energy of such a system, close to equilibrium, that has been extended linearly to nonequilibrium conditions.⁶ Here electrochemical potential may be considered to be the same as the chemical potential as discussed in footnote a.³

The goal of this investigation is to develop a mathematical formalism that facilitates interpretation of kinetic rates and changes in thermodynamic free energies for an energy-time curve such that it

^a Electrochemical potential measured in a two electrode cell may be expressed⁷ as $\Delta V = V_1(\text{electrode1}) - V_2(\text{electrode2}) = (E_1 - \psi_{\text{ewf}}) - (E_2 - \psi_{\text{ewf}})$ where ψ_{ewf} is the energy required to remove an electron from an electrode surface to a vacuum; this is also known as the electron work function and has a value of -4.6 ± 0.1 eV. The electron work function (EWF or absolute) may be considered to be a reference energy. Electrochemists prefer to use a normal hydrogen electrode (NHE), a calomel electrode, or a silver chloride electrode as a reference potential. The NHE value is taken to be 0.00 V, and is actually a relative reference-4.6 V different from the EWF value, and is applied to all measured electrochemical potential values. Thus, the electrochemical potential of aluminum of -1.662 V is relative to the standard NHE or $+3.062$ V absolute. The electrochemical potential of an electron in a metal is its Fermi energy while the Fermi energy of a semiconductor may be the average of the valence band energy and the conduction band energy. Once equilibrium has been established the electrochemical potential⁸ may be considered to be the same as the chemical potential.

^b It is necessary to consider the relationship between thermodynamic chemical potential and electrochemical potential. The energy state of an ion in solution is primarily composed of the sum of short range ionic interactions and a long range energy field required to establish the potential charge of the ion.⁶ Thus, the electrochemical potential, μ_i , is a sum of the standard chemical potential, μ_i° , and the potential resulting from local ionic species, ϕ , as $\mu_i = \mu_i^\circ + z_i \mathcal{F} \phi$ where $\mu_i^\circ = (\partial F / \partial n_i)_{T,P,n_j}$, \mathcal{F} is Faraday's constant, and z_i is the ionic charge on component i . For a pure phase at unit activity the electrochemical potential $\mu_i = \mu_i^\circ$, the chemical potential. For equilibrium species i between phases α and β , $\mu_i^\alpha = \mu_i^\beta$ implying that the terms containing potential ϕ become equal making a null contribution to the equation. Thus, for a state of equilibrium especially for dilute solutions, a chemical potential may be considered to be the same as an electrochemical potential. Constant open circuit potentials (OCPs) measured at $i_{\text{OCP}} = 6 \times 10^{-9}$ A, as reported in the previous article, are considered to be near equilibrium chemical potentials since the current, which is a measure of change in charge or concentration with time, is small.

² E-mail: mcarter@ektech.com

reveals the underlying chemistry. It becomes apparent that each chemical reaction equation in the system is represented by one reaction rate and one chemical potential. These values may be considered to be equation constants once all mutually interdependent reaction information is accounted for, that is, when the system approaches equilibrium.^c Such a system may be considered to be in compliance with the second law of thermodynamics³ when current flow associated with an OCP is low and approaches zero.

Mathematical Considerations

Detailed chemical and electrochemical disclosure was made in the previous article¹ showing an OCP curve for aluminum immersed in IC remover chemistry that consisted of three separate and distinct functions modeled as a set of sequential chemical reaction equations. They are (i) dissolution of the native surface oxide, (ii) reaction of aluminum metal with water, and (iii) repassivation of the exposed aluminum metal surface. This electrochemical process may be treated as a system. In addition, it has become clear that some of the reactions in the system were interdependent on other reactions in the set so as to produce sufficient concentrations of critical intermediate chemical components in order for the whole process to proceed to a final steady state over time.

An OCP graphical figure represents changes in potential caused by combining reactive components. For example, oxidation of aluminum metal by water produces an OCP of -1.66 V. This circuit potential is a direct result of the chemical changes that occur naturally. Thus, this chemical system exhibits a negative change in free energy, a changing potential for chemical rebalance as the system proceeds toward equilibrium. Time-dependent changes of free energy indicate changing chemical composition. Development of a time-dependent free energy equation, for times τ long compared to the time of electron transport approximated by $t_t = (d/c)$ between electrodes (times longer than $1-2$ s, for electrode spacing d and velocity of light c , such that $\tau \gg t_t$ for a system of chemical reactions proceeding toward thermodynamic equilibrium, follows.

Consider a dilute chemical system of sequential reactions that proceed slowly in time (requiring more than a few seconds). A system consisting of two well-mixed dilute solutions or a dilute solution exposed to a few atomic layers of a chemically active surface proceed toward a state of thermodynamic equilibrium. The partial differential molal free energy of such a system is given in terms of the thermodynamic³ equation of state as

$$dF = (\partial F/\partial T)dT + (\partial F/\partial P)dP + \sum_i (\partial F/\partial n_i)dn_i \quad [1]$$

$$= -SdT + VdP + \sum_i \mu_i dn_i \quad [2]$$

where μ_i is the chemical potential (Fermi level⁸) of component i . At the normal conditions of constant T and P the differential expression becomes $dF = \sum_i \mu_i dn_i$ or $dF = \mathcal{F} \sum_i \mu_i' dn_i$ where \mathcal{F} is Faraday's constant and $\mu_i = \mathcal{F}\mu_i'$.

A state of equilibrium is expressed by $\Delta F \approx 0$, corresponding to zero applied potential, and becomes a boundary condition for mathematical treatment. In addition, it is required that (dF/dt) approach zero. Conservation of mass is chosen as another limiting condition

^c The possibility that the closed electrochemical system treated in this work may be an irreversible thermodynamic system has been considered. Initial components, their concentrations and thus their equilibrium constants, are interrelated and are not defined as independent entities with restricted phase space. In addition, experimental data demonstrated the interrelationship of the products. Thus, the chemical system may be considered as deterministic and not probabilistic. Furthermore, closed electrochemical systems may be shown to be chemically reversible systems allowing for a consumption of energy and an increase in entropy. From a chemical viewpoint the system is considered to be reversible but from an energy viewpoint it is considered to be irreversible as, of course, real world thermodynamic systems are.

where the total mass of the system is constrained. Inclusion of, for example, one component of solvent and $i - 1$ components of solute results in a total mass of unity defined as

$$\sum_i M_i n_i = 1 \quad [3]$$

where n_i is the number of moles of the i th component per 1000 g and M_i is the molecular weight of the i th component.^d The masses are determined by the chemical equations derived from single-electron electrochemical reactions. For example, the chemical equation for iodine oxidation of ferrocyanide may be written as two single electron half cell reactions, namely $\text{Fe}(\text{CN})_6^{4-} \rightarrow \text{Fe}(\text{CN})_6^{3-} + e^-$ and $1/2\text{I}_2 + e^- \rightarrow \text{I}^-$. The masses are the molecular weights of the products as shown.

The differential free energy equation expresses interaction between one molal component, i , and the others, j . This relation enters naturally as a partial differential expression in

$$dF = \sum_{i \leq j} (\partial F/\partial n_i)(\partial n_i/\partial n_j)dn_j = \mathcal{F} \sum_{i \leq j} \mu_i' (\partial n_i/\partial n_j)dn_j \quad [4]$$

where the sum is taken for i being 1 to ℓ and j being from i to ℓ so duplication of indexes is avoided. The concentration of chemical component i may be represented by a negative exponential function of time as

$$n_i = \eta_i a \exp(-\omega_{ij}t) \quad [5]$$

where η_i is the initial molal concentration of component i (at $t = 0$) for an ℓ component set ($1 < i < \ell$), a is the constant pre-exponential factor and ω_{ij} is a frequency factor. Real-time-based asymptotic functions, like Bessel functions that appear in a wide variety of physical problems,⁹ represent the rate functionality that accompanies chemical potential. Interaction between two such functions of n_i and n_j may be represented by the binary expression

$$(n_i/n_j) = [\eta_i a \exp(-\omega_{ij}t)]/[\eta_j a \exp(-\omega_{ji}t)] \quad [6]$$

The change in free energy of the system with time may be expressed by the differential equation

$$dF/dt = \mathcal{F} \sum_{i \leq j} \mu_i' (\partial n_i/\partial n_j)dn_j/dt \quad [7]$$

Equation 6 is expressed as a differential equation in time in terms of the binary molal concentration function as

$$(\partial n_i/\partial n_j) = (\partial n_i/\partial t)/(\partial n_j/\partial t) = (\eta_i \omega_{ij}/\eta_j \omega_{ji}) \exp(\omega_{ji}t - \omega_{ij}t) \quad [8]$$

and

$$(dn_j/dt) = -\eta_j a \omega_{ji} \exp(-\omega_{ji}t) \quad [9]$$

The time-based free-energy expression, substituting expressions 8 and 9 into Eq. 7, becomes

$$\begin{aligned} dF/dt &= \mathcal{F} \sum_{i \leq j} \mu_i' (\partial n_i/\partial n_j)dn_j/dt \\ &= -\mathcal{F} \sum_{i \leq j} \mu_i' \eta_i a \omega_{ij} \exp(-\omega_{ij}t) \end{aligned} \quad [10]$$

^d A more precise definition of the conservation of mass is $\sum_i M_i n_i = b$ where b is a constant and $b = 1$ for a total mass of 1000 g s. However, by redefining the units of n_i to be other values, such as moles per 1 g or moles per 10 g, then the constant is still $b = 1$.

The constant a is readily evaluated from Eq. 5. By setting $t = 0$ it may be observed that $\eta_i = n_i$ so $a = 1$. The constant term, a , is also determined by the conservation of mass condition, $\sum_{i=1}^l M_i \eta_i a \exp(-\omega_i t) = 1$. At $t = 0$ then $\sum_{i=1}^l M_i \eta_i a = 1$ and the constant may be expressed as

$$a = \sum_i (1/M_i \eta_i) \quad [11]$$

but $\sum_i M_i \eta_i$ also sums to 1, thus $a = 1$ and the free energy expression 10 becomes

$$dF/dt = -\mathcal{F} \sum_{i=1}^l (\eta_i \mu_i' \omega_i) \exp(-\omega_i t) \quad [12]$$

Each expression in i contains all of the rate-related terms. This equation can be simplified by letting $\kappa = \sum_i \omega_i$, a sum of constants, so $dF/dt = -\kappa \mathcal{F} \sum_i (\eta_i \mu_i') \exp(-\omega_i t)$. Integration produces an equation for limited change in free energy of the system in a region near equilibrium as

$$\begin{aligned} \Delta F(t) &= -\kappa \mathcal{F} \sum_i \eta_i \mu_i' \int \exp(-\omega_i t) dt \\ &= \kappa \mathcal{F} \sum_i \eta_i \mu_i' [(1/\omega_i) \exp(-\omega_i t)]_0^t \\ &= \kappa \mathcal{F} \sum_i \eta_i \mu_i' \{[(1/\omega_i) \exp(-\omega_i t)] - (1/\omega_i)\} \quad [13] \end{aligned}$$

where the constant $-\sum_i (1/\omega_i) = -(1/\kappa)$ is ignored as small. The integral form of free energy equation 13 meets the equilibrium condition as time approaches the time of the measurement when the change in $\Delta F(t)$ with time approaches zero. The index i is the number of chemical reaction components in the system represented by one equation per chemical reaction and a solution is accomplished for a set of such equations as one equation per unknown. Thus, one unknown is allowed per component, either the reaction rate, ω_j , or the chemical potential, μ_j' . The equation $\Delta F(t)$ represents a set of linear equations which if solved as a matrix would be solved simultaneously. Instead, Eq. 13 is solved as a sum of sequential equations to facilitate determination of the constants by fitting to a specific experimental curve.

Consider $\Delta F(t)$ to be a real function of rate ω_j and chemical potential μ_j' . If this function is able to be differentiated at $t = 0$ and in a small region about $t = 0$ such that, if no singularity exists for $d\Delta F(t)/dt$, then $\Delta F(t)$ is analytic¹⁰ at $t = 0$. A smooth, continuous field of such points may be considered in a well-defined region about t such that, if no singularity exists for $d\Delta F(t)/dr$, then $\Delta F(t)$ is analytic throughout this region. A solution of the sum of sequential equations is sought by determining the unknown constants upon fitting the experimental OCP curve.

The frequency factors, ω_j , present in (dn_j/dt) expressions are inherently first-order rate constants but may be related to apparent second-order rate constants. Here a reaction rate expression may be stated as $dC_a/dt = -k_a C_a$ or expressed in terms of molal concentration $(dn_j/dt) = -k_j n_j$ where $n_j = \eta_j a \exp(-\omega_j t)$ and $(dn_j/dt) = -\eta_j a \omega_j \exp(-\omega_j t)$ as before. Solving for the rate constant lets

$$k_j = \omega_j \quad [14]$$

where rate constants may be expressed in units of 1/s. An apparent second-order rate constant may be expressed as

$$k_j = (\omega_j M_j / 1000 \rho) \quad [15]$$

in units of L/mol-s where M_j is the molecular weight of the j th component and ρ is the density of the solution. Mathematical Eq. 5

through 13 contain time-based expressions, however, the reaction order is ultimately determined by extracting the sum or product of equilibrium constants related to chemical reaction model equations and are typically constant during the time of reaction.

Rate constants and accurate chemical potentials for industrial reactions in a condensed state are often unavailable. Numerous measured values have been reported determining kinetic values for selected gas-phase reactions¹¹ and reaction rates can be estimated for gases from thermodynamic data. For other cases where the rate constants or chemical potentials are not available, that is when the number of unknowns exceeds ℓ , a semiempirical approach, as guided by application of Eq. 13, may be possible. However, the total number of unknown values is limited to less than the number of experimental data points. Reasonable results may be obtained by an iterative minimization of deviations (regression analysis) approach to match Eq. 13 to experimental curves. Semiempirical computations are readily facilitated for Eq. 13 expressed as

$$\begin{aligned} \Delta F(t) &= \mathcal{F} \sum_r (\omega_1 + \omega_2 + \dots + \omega_l) (\eta_r \mu_r' / \omega_r) \exp(-\omega_r t) \\ &= \mathcal{F} \sum_r \kappa \eta_r (\mu_r' / \omega_r) \exp(-\omega_r t) = \sum_r (c_r / \omega_r) \exp(-\omega_r t) \quad [16] \end{aligned}$$

where

$$c_r = \mathcal{F} \kappa \eta_r \mu_r' \quad [17]$$

and where the index i has been replaced by the index r to identify reaction r that contains chemical component i . Active redox reactions usually drive the generation of experimental OCP curves. However, it is recognized that the constants μ_r' and ω_r also relate to active chemical component i those minimally active and ion exchange species necessary to complete the reaction set but whose chemical potentials are usually minimal (close to zero). Thus, $\Delta F(t)$ produces a pair of constants, c_r (a function of chemical potential) and ω_r (reaction rate), for each underlying chemical reaction upon fitting an experimental curve. These pairs of constants identify the type of chemical reaction acting and individual reactions may be specified through knowledge of the chemicals present. Should the model chemical reactions not be rationalized with the constants generated by the curve fitting procedure then another set of model chemical reactions should be found until agreement is attained.

Experimental Measurements

OCP measurements were conducted to record changes in potential with time for oxidation of ferrocyanide ion by iodine from a KI_3 complex. To 13 mL of 18.2 mM solution of $K_4Fe(CN)_6$ stirred at 500 rpm was injected 50 μ L of 55 mM KI_3 solution. Fresh $K_4Fe(CN)_6$ solutions were prepared often and kept sealed between uses. Three sets of measurements were conducted at $22 \pm 2^\circ C$ and atmospheric pressure for this reaction but the concentration of the ferrocyanide ion was difficult to control due to its propensity for rapid air oxidation. Measurements were conducted using a computer-controlled Solartron 1287 electrochemical interface, using Scribner software, for a closed glass cell consisting of two nitric acid-cleaned platinum foil electrodes, a saturated Ag/AgCl reference electrode, a micromagnetic stir bar, and a nitrogen gas bubbler. Each solution was stirred at 500 rpm under nitrogen gas for less than 3 min while the electrochemical baseline stabilized and 50 μ L of 10 mM KI_3 (prepared by dissolving 0.2538 g of I_2 in 150 mM KI solution and diluting to 100 mL) was injected just above the liquid surface⁶ to initiate the reaction. Perturbation due to the injection

⁶ The electrochemical cell could become grounded if contacted by the needle thereby invalidating the measurement.

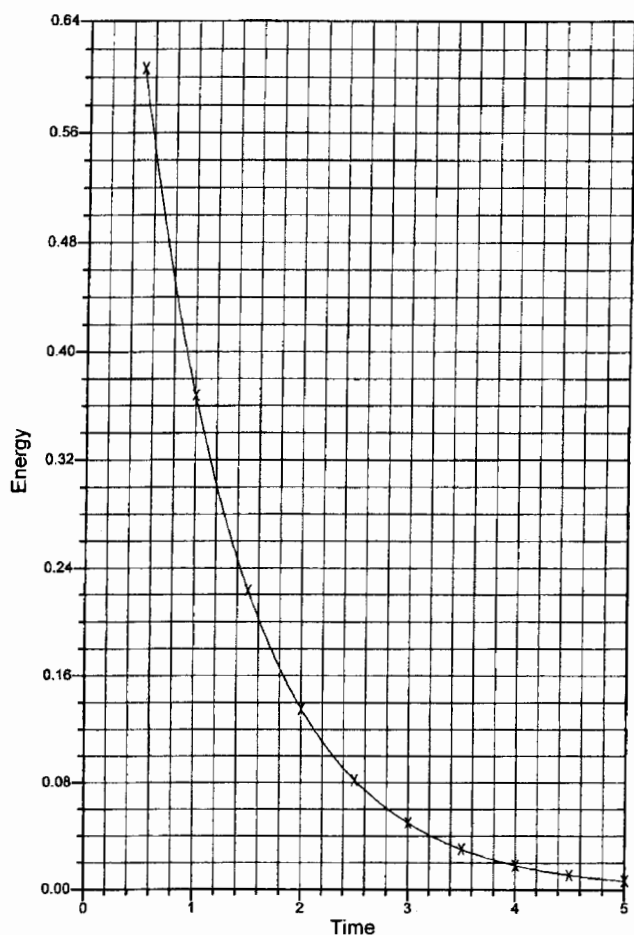


Figure 1. Computed curve to match mathematical table e^{-x} values.

caused an increase in potential lasting 2 s followed by a smooth decline in potential that was completed in less than 3 min. Refer to Fig. 2a for a sample OCP curve.

OCP measurements were conducted for aqueous formula FB that contained 70 wt % *N*-dimethylformamide and 30 wt % of an aqueous solution of 27 mmol of diisopropylethylquaternaryammonium fluoride adjusted to pH 9 with an alkylamine by immersing an aluminum working electrode 1 cm from a platinum counter electrode and immediately initiating the measurement. Results of potential were recorded as a function of time for 400 s where the resultant current drain was 6 ± 1 nA/cm². Refer to Fig. 3a. Removal (corrosion) of the 570 nm aluminum film continued at -1.66 V until the film was completely dissolved.

OCP measurements were also conducted for formula FA (similar to formula FB except ammonium fluoride replaced the quaternary) by immersing an aluminum working electrode 1 cm from a platinum counter electrode and immediately initiating the measurement. The initial potential of -1.3 V changed in some 40 to 50 s to -1.66 V where it remained until an elapsed time of 100 s and then abruptly changed approaching -0.7 V after some 400 s. Here again the re-

Table I. Data points from mathematical table e^{-x} values.

Time (s)	Potential (V)	Time (s)	Potential (V)
0.5	0.60653	3.0	0.04979
1.0	0.36788	3.5	0.03020
1.5	0.22313	4.0	0.01832
2.0	0.13534	4.5	0.01111
2.5	0.08208	5.0	0.00674

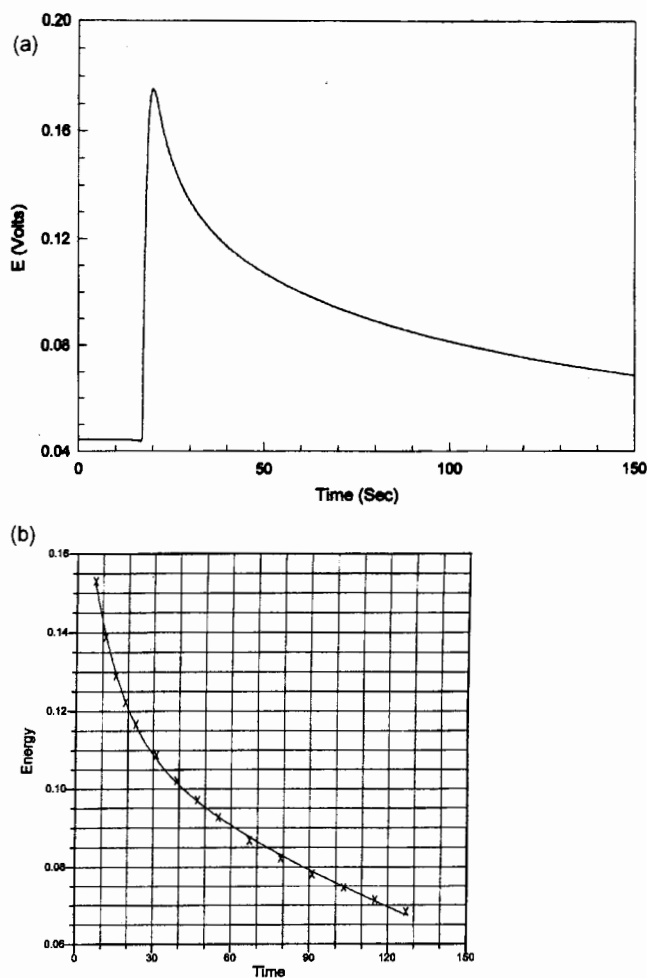


Figure 2. (a, top) OCP of $K_4Fe(CN)_6 + I_2$. (b, bottom) Computed OCP of $K_4Fe(CN)_6 + I_2$ curve and data points.

sultant current drain was 6 ± 1 nA/cm². Refer to Fig. 4a. Removal (corrosion) of the thin aluminum film was abated as the film became passivated.

Table IIA. Sample data points from OCP of $K_4Fe(CN)_6 + I_2$.

Time (s)	Potential (V)	Time (s)	Potential (V)	Time (s)	Potential (V)
7.1	0.153	31.1	0.109	79.1	0.0823
11.1	0.139	39.1	0.102	91.1	0.0782
15.1	0.129	47.1	0.0971	103.1	0.0747
19.1	0.122	55.1	0.0927	115.1	0.0715
23.1	0.117	67.1	0.0869	127.1	0.0684

Table IIB. Computed chemical potentials and reaction rates for OCP of $K_4Fe(CN)_6 + I_2$.

ℓ	r	c_r NLREG	Chemical potential μ_r' (V)	ω_r (l/s)	k_r (L/mol s)
2	1	5.637×10^{-3}	0.358	0.0112 ± 0.0016	0.00237
2	2	4.052×10^{-2}	0.538	0.1084 ± 0.0026	0.0137

Here 1 represents $Fe(CN)_6^{4-}$ and 2 represents I^- .

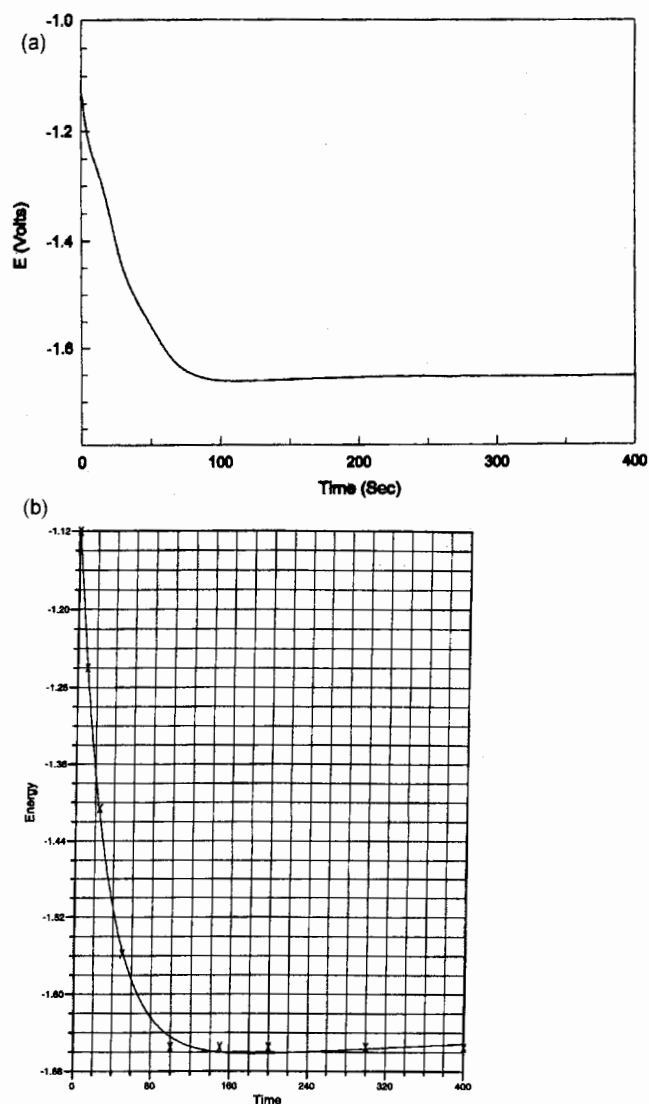


Figure 3. (a, top) OCP of quateramine formulation FB. (b, bottom) Computed OCP of quateramine formulation FB curve and data points.

Discussion

The goal of this effort was to interpret experimental OCP curves in terms of a causal chemical reaction model by a computational method consisting of three logical steps. First, Eq. 16 was solved for an OCP figure by means of a regression analysis curve fitting routine adjusting the number of terms that represent the minimum number of chemical reactions acting and to compute a pair of constants, chemical potential, and reaction rate, for each reaction. Second, a model set of reactions was expressed based on knowledge of the chemical compounds present in an effort to explain the chemical basis for the OCP. Finally, the chemical reaction model was compared with the computed constants to determine if the model was in reasonable agreement with the mathematical analysis of the data. For example, a computed chemical potential of -1.66 V would confirm dissolution of aluminum metal, a chemical potential of -0.45 or -0.037 V might indicate that iron metal was active and $+0.34$ V could indicate that copper was active. For those more complex chemical situations where insufficient data was available a semiempirical approach may be employed by estimating starting values for some reaction rate constants ω_r , remembering that solving for r equations allows for not more than r unknown values.

Table IIIA. Data points from OCP of formulation FB.

Time (s)	Potential (V)	Time (s)	Potential (V)	Time (s)	Potential (V)
1	1.32	50	1.76	200	1.85
10	1.46	100	1.85	300	1.85
25	1.61	150	1.85	400	1.85

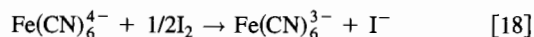
Table IIIB. Computed chemical potentials and reaction rates for OCP model of formulation FB.

1	r	Reaction no.	c_r NLREG	Chemical potential μ'_r (V)	ω_r (l/s)	k_r (L/mol s)
4	1	19	0.0001	5.57×10^{-8}	396.	14.7
4	2	20	-1.304×10^{-7}	-7.27×10^{-11}	3.20×10^{-5}	1.44×10^{-6}
4	3	21	4.479×10^{-5}	2.50×10^{-8}	0.0321	8.97×10^{-4}
4	4	22	-2.953.	-1.65	17.1	0.460

Assumed values may be adjusted until the regression analysis returns computed values that provide the best fit to experimental curves.

The degree of accuracy provided by the NLREG computational routine (available on the web) was determined by fitting constants c_r and ω_r of Eq. 16 to a set of ten five place e^{-x} values from a mathematical table¹² (c_r , ω_r , and η_r were set to 1.000000 initially), refer to Fig. 1. The algorithm was run on a Sony notebook computer using Eq. 16 until a minimization of the sum of squared deviations or residuals of the function was achieved. It returned the acceptable values of $\omega_1 = 0.999992$ and $c_1 = 1.00001$ indicating five figure accuracy. Refer to data Table I for the data points used.

OCP curves were recorded for a specific redox reaction chemistry specified by the two chemical half-cell reactions $\text{Fe}(\text{CN})_6^{4-} \rightarrow \text{Fe}(\text{CN})_6^{3-} + e^-$ and $1/2\text{I}_2 + e^- \rightarrow \text{I}^-$ resulting in chemical Eq. 18 as



where iron (II) became oxidized to iron (III) by iodine, refer to Fig. 2a and Table IIA for the average of three sets of experimentally measured data. Regression analysis was conducted using starting chemical potentials of $\mu'_1 = 0.358$ V and $\mu'_2 = 0.538$ V, that matched the data of Fig. 2a for $\ell = 2$, refer to Fig. 2b for the matched data curve. The X symbols on the figure represent measured data points, and the solid line was the computed curve for constants presented in Table IIB. The concentrations, η_r , were taken from the prepared solutions presented in the experimental section.

The resulting computed rate constants were $\omega_1 = 0.011 \pm 0.002/\text{s}$, for oxidation of $\text{Fe}(\text{CN})_6^{4-}$ to $\text{Fe}(\text{CN})_6^{3-}$ and $\omega_2 = 0.108 + 0.003/\text{s}$ for reduction of I_2 to I^- . The values of $c_r = \mathcal{F}k_r\eta_r\mu'_r$ returned yielded values of $\mu'_1 = 0.358$ V and $\mu'_2 = 0.538$ V in agreement with the literature values¹³ of 0.358 V for the oxidation potential of the $\text{Fe}(\text{CN})_6^{4-}$ ion and 0.536 V for the oxidation potential of the I_2 . Rate constants¹⁴ of 0.014 ± 0.002 cm/s and 0.011 ± 0.002 cm/s have been reported¹⁵ for reduction of $\text{Fe}(\text{CN})_6^{4-}$ ion using a microcylindrical carbon electrode and systematic variations of electrodes, solvents, and temperature on the redox potential have also been reported.¹⁶⁻²¹ The derived value of constant ω_1 was in agreement with these reported values. Limited I_2 reaction rate data reported a recombination rate²² for $\cdot\text{I}_2^-$ of 3.2×10^9 L/mol s for a free radical version of this reactant but a directly comparable rate value was not found. Results of the experimental

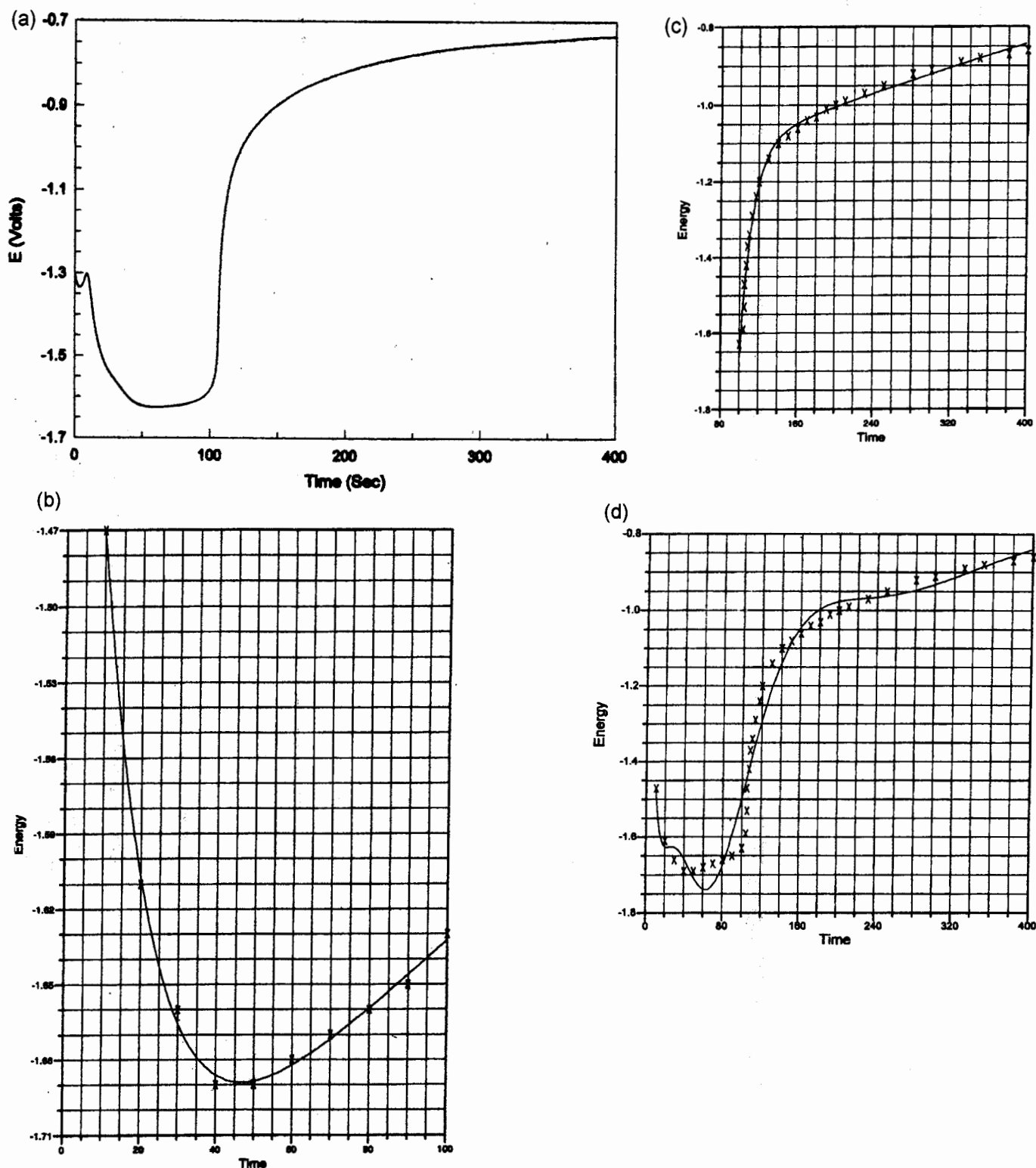


Figure 4. (a, top left) OCP of ammonium fluoride formulation FA. (b, top right) Computed OCP of 0 to 100 s of ammonium fluoride formulation FA curve and data points. (c, bottom left) Computed OCP of 100 to 400 s of ammonium fluoride formulation FA curve and data points. (d, bottom right) Computed OCP of ammonium fluoride formulation FA curve and data points.

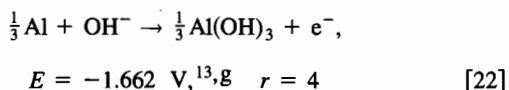
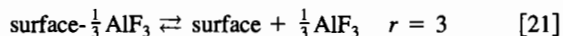
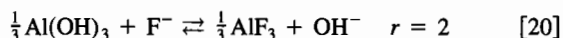
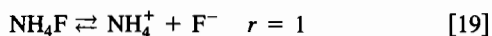
method of reacting $\text{Fe}(\text{CN})_6^{4-}$ with I_2 were sufficiently repeatable to produce the reported chemical potentials and the one reported reaction rate suggesting the time-dependent free energy formalism to be useful.

A series of OCPs were recorded for immersion of a 570 nm thick aluminum metal film on a silicon wafer coupon in a solution of

formula FB, refer to Fig. 3a. The NLREG was conducted for the OCP of Fig. 3a (data Table IIIA), for $\ell = 3$, with c_1 set to 0.0001, c_2 set to 0.38, and the chemical potential μ_4 (μ_3 was omitted) initially constrained to -1.662 V, but no quantitative solution was found. Refer to chemical reaction Eq. 19 through 22. Increasing the equation set to $\ell = 4$ and assuming all concentration distributions

η_r , to be equal to 4.5×10^{-5} for this very dilute chemistry,^f setting starting chemical potentials as above, ω_1 to near 400, c_1 to 0.0001 V and c_2 to 0.38 where μ_4' was set to -1.662 V produced the anticipated results; refer to X marks in Fig. 3b and values in Table IIIB.

The aluminum dissolution chemistry has been modeled by the four chemical reactions identified below as Eqs. 19-22



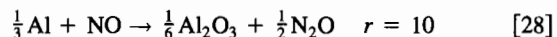
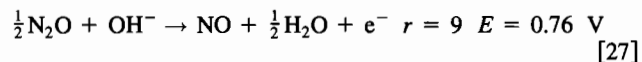
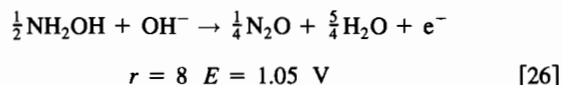
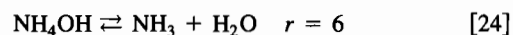
Reaction 19 generated an equilibrium concentration of fluoride ion, Reaction 20 replaced surface metal hydroxide by fluoride, Reaction 21 allowed for dissolution of the aluminum fluoride surface so oxidation of the aluminum metal surface, Reaction 22, could proceed. Since no metal passivation mechanism was active this reaction continued until the aluminum film became completely dissolved.

Computed results for the $\ell = 4$ equation set not only fit the OCP curve but a correct value of c_4 , the critical driving Reaction 22, was returned; refer to data presented in Table IIIB. Computed values for an apparent equilibration reaction were $\mu_1' = 5.57 \times 10^{-8}$ V with a reaction rate of $\omega_1 = 396/\text{s}$ ($k_1 = 14.7$ L/mol s). Chemical potentials of μ_2' of -7.27×10^{-11} V and μ_3' of 2.50×10^{-8} V were insignificant compared to the value of μ_4' , as were the reaction rates of $\omega_2 = 3.20 \times 10^{-5}/\text{s}$ ($k_2 = 1.44 \times 10^{-6}$ L/mol s) and $\omega_3 = 3.21 \times 10^{-1}/\text{s}$ ($k_3 = 8.97 \times 10^{-4}$ L/mol s). Chemical Eq. 22 was represented by a chemical potential of μ_4' of -1.65 V¹³ and a rate constant of $\omega_4 = 17.1/\text{s}$ ($k_4 = 0.460$ L/mol s). This data confirms chemical Eq. 22 as the driving reaction. Nonetheless, this application required four sets of reaction constants to match the experimental OCP curve, and the set of model Eq. 19, 20, 21, and 22 matched that requirement.

The mathematical formalism provided results for four pairs of constants for aluminum immersed in formula FB, but it was not known if this mathematical analysis process could successfully model a more complex OCP. Equation 16 was applied to the convoluted OCP of aluminum immersed in formula FA, see Fig. 4a, using a semiempirical approach and data points of Table IVA. The initial curve analysis was conducted in two distinct parts for partial time segments to estimate the chemical potential and reaction rate constants. These estimated values of chemical potentials and frequency factors were applied as initial values for a new analysis of the entire 400 s curve. First Eq. 16 was applied to the 0 to 100 s segment, up to the plateau of the OCP, using a four-parameter process ($\ell = 4$ for Reactions 19, 20, 21, and 22) starting with results of Table IIIB and setting η_r to 4.5×10^{-5} M as before. Refer to the results in Table IVB and Fig. 4b. A three-variable set did not produce an acceptable solution, but a four-variable set did optimize the degree of curve fit and provided the expected value of μ_4' . Next Eq. 16 was applied to the 100 to 400 s segment of the curve, from the plateau to the end of the OCP curve of Fig. 4a using the data of Table IVA as initial values for a four-parameter process ($\ell = 4$ for Reactions 25, 26, 27, and 28). Again a four-variable set did produce

a reasonable curve fit, refer to the results in Table IVB and Fig. 4c. The chemistry of the complete OCP (0 to 400 s) was then modeled by incorporating the major values of the previous two truncated data sets as starting values in a new computation for $\ell = 8$ and above maintaining η_r at 4.5×10^{-5} as before. Approximate computational solutions were found using eight and ten sets of variables. Refer to Fig. 4d and results in Table IVB for the OCP curve and computed results. The $\ell = 8$ parameter set did approximate the curve of Fig. 4a, but the limited set produced a zero slope beyond 200 s instead of the non-zero slope as shown in Fig. 4a. This also indicated that more than eight parametric equations were required to produce a better curve fit. Variations in the quality of the curve fitting were affected by changes in the constant c_r but the frequency factors, ω_r , changed only slightly. Pursuit of acceptable results for the $\ell = 8$ and $\ell = 10$ data sets required numerous attempts via small changes in starting values for the NLREG algorithm before an approximate fit was achieved, yet the NLREG software readily computed acceptable results for $\ell = 2$ to 4 with a wide range of starting data. This indicated a weakness in the regression analysis approach for $\ell > 4$.

Immersion of aluminum metal into remover chemistry formula FA, that produced the OCP of Fig. 4a, was modeled by a ten chemical reaction equation set of Eq. 19 through 28



Dissolution of the active aluminum surface, 22, generated a negative potential (cathode) so the oxidation steps Eq. 26 and 27 may have occurred at the counter electrode (anode). Table IVB, data set for $\ell = 10$, indicated chemical Eq. 19 could fit the chemical potential and rate-constant parameters of $\mu_1' = 1.14 \times 10^{-8}$ V and $\omega_1 = 1.19 \times 10^4/\text{s}$ different from the data of Table IIIB and $\ell = 8$ sets in Table IVB (negative rate values imply a reversed reaction). Here a near-zero chemical potential would indicate equilibrium and a high value of the frequency factor would indicate rapid attainment of equilibrium expected for Reaction 19. A similar set of values was computed for chemical Eq. 24 where $\mu_6' = 1.44 \times 10^{-8}$ V and $\omega_6 = 1.20 \times 10^4/\text{s}$. Here the equilibration rates and the chemical potentials were similar to those for $r = 1$. The initial chemical potential of Eq. 22 was set to -1.662 V for the dissolution (corrosion) of aluminum metal in a mildly alkaline solution and a value of -1.662 V was returned while an apparent rate constant of $\omega_4 = 1.90 \times 10^{-5}/\text{s}$ was computed. Chemical Eq. 26 for electrochemical conversion of hydroxylamine to nitrous oxide was represented by the values of $\mu_8' = 1.07$ V and $\omega_8 = 2.78 \times 10^{-3}/\text{s}$ close to the estimated chemical potential of 1.05 V. Chemical Eq. 27, representing reoxidation of nitrous oxide to nitric oxide, produced a value of $\mu_9' = 0.77$ V with a rate constant of $\omega_9 = 5.40 \times 10^{-3}/\text{s}$ close to a reported redox potential of 0.76 V.¹¹ Chemical Eq. 20 may be viewed as an exchange reaction with a $\mu_2' = 1.20 \times 10^{-2}$ V and $\omega_2 = 4.97 \times 10^{-2}/\text{s}$. Chemical Eq. 21 represents dissolution of the passivated surface with a $\mu_3' = 3.90 \times 10^{-2}$ V and $\omega_3 = 4.66 \times 10^{-2}/\text{s}$. Chemical Eq. 23 established an alternative condition for potential dissolution of the passivating film with $\mu_5' = -5.20 \times 10^{-2}$ V and $\omega_5 = 4.74 \times 10^{-2}/\text{s}$. Chemical Eq. 25

^f Since $\Delta F = 0$ and since all concentration factors $\eta_r = 1$, the computed values will be essentially the same as for $\eta_r = 10^{-3}$ or 10^{-6} .

^g The half reaction listed in Ref. 12, $1/3\text{Al} \rightleftharpoons 1/3\text{Al}^{3+} + \text{e}$, is suspect. Two half reactions are expected to add together to form one complete chemical reaction as $1/3\text{Al} + \text{OH}^- \rightleftharpoons 1/3\text{Al}(\text{OH})_3 + \text{e}^-$ and $\text{H}^+ + \text{e}^- \rightleftharpoons 1/2\text{H}_2$ to yield (as multiplied by 3) $\text{Al} + 3\text{H}_2\text{O} \rightleftharpoons \text{Al}(\text{OH})_3 + 3/2\text{H}_2$. Since water is a necessary part of the aluminum reaction sequence the later aluminum half reaction has been expressed in this work.

Table IVA. Data points from OCP of formulation FA.

Time (s)	Potential (V)	Time (s)	Potential (V)	Time (s)	Potential (V)
0	1.40	105	1.47	180	1.03
10	1.47	107	1.42	190	1.01
20	1.61	108	1.37	200	1.00
30	1.66	110	1.34	210	0.99
40	1.69	113	1.29	230	0.97
50	1.69	117	1.24	250	0.95
60	1.68	120	1.20	280	0.92
70	1.67	130	1.14	300	0.91
80	1.66	140	1.10	330	0.89
90	1.65	150	1.08	350	0.88
100	1.63	160	1.06	380	0.87
104	1.59	170	1.04	400	0.86
104.5	1.53				

represents the possible reaction of ammonia with a $\mu_7' = -0.614$ V and $\omega_7 = 5.67 \times 10^{-3}/s$ while chemical Eq. 28 represents formation of a thin film of insoluble aluminum oxide with a $\mu_{10}' = -1.18 \times 10^{-2}$ V and $\omega_{10} = 3.06 \times 10^{-3}/s$. Figure 4d showed the computed curve did approximate the measured data points but not overlay them. Computations conducted for all values constrained to those values believed to be correct did cause the computation to halt prior to completion. Possibly a more quantitative minimization algorithm could improve the curve fit computation for $\ell > 4$. Nonetheless, the computed constants did approximately represent the chemical reaction equations indicating chemical Eq. 19 through 28 represented a reasonable model of aluminum surface corrosion in remover FA.

The mathematical results of Table IVB did show there were at least five main chemical equations, one for each large value of a

constant. However, it was shown that each partial curve fitting required a minimum of four parameters for the 0 to 100 s region and at least four parameters for the 100 to 400 s region so that a minimum set of eight chemical reaction equations were required to satisfy the aluminum surface-cleaning model responsible for production of the OCP of Fig. 4a. Furthermore, a zero slope computed for the OCP in the 200 to 400 s region for $\ell = 8$ indicated that ℓ was greater than 8. The additional equations with smaller constants serve to refine the chemical model.

A quite limited number of chemicals were present initially¹ in the experiments performed. They consisted of a passivated aluminum metal surface, water, a water soluble organic solvent such as dimethylformamide (DMF), less than two percent ammonium fluoride and a fractional percent concentration of an amine to adjust pH. This picture became somewhat more complex as Al became exposed and corroded, AlF_3 formed, and some NH_3 became vaporized in an equilibrium shift. In addition, a minor amount of ammonia may have been oxidized and low concentrations of impurities could have participated.

Reactions capable of producing a potential significantly different from zero involve redox, that is reduction-oxidation chemistry usually associated with a low level of electrical current for reactions close to equilibrium. Once a potential field has been established, chemical reaction equations that modify the potential as a function of time may also participate. For example, exposure of a passivated aluminum metal surface to an aqueous solution might result in a measured potential of -1.3 to -1.4 V where water can react with aluminum via a resistive, porous native oxide layer. Should a secondary chemical reaction proceed to remove this passivation layer then the measured potential would be anticipated to change to -1.66 V as observed, the redox potential for aluminum in water, as seen in Fig. 3a and 4a. In this case chemical reactions directing both removal of the passivating film and oxidation of the aluminum were

Table IVB. Computed chemical potentials and reaction rates for OCP of formulation FA.

l	r	c_r NLREG	Chemical potential μ_r' (V)	ω_r (1/s)	k_r (L/mol s)	M_r (Daltons)	Comments
4	1	0.0001	5.57×10^{-8}	396.	14.7	37.04	Fit to 0–100 s of Fig. 4a
4	2	-1.30×10^{-7}	-7.27×10^{-11}	3.20×10^{-5}	1.44×10^{-6}	44.98	
4	3	4.48×10^{-5}	2.50×10^{-8}	0.0321	8.97×10^{-4}	27.93	
4	4	-2.953	-1.65	17.1	0.460	26.91	
4	5	0.0001	5.57×10^{-8}	396.	13.9	35.04	Fit to 100–400 s of Fig. 4a
4	6	-4.22×10^{-7}	-1.10×10^{-10}	2.45×10^{-4}	8.24×10^{-6}	33.55	
4	7	2.474	1.38	0.328	1.28×10^{-2}	39.01	
4	8	-2.30	-1.28×10^{-3}	0.0946	3.69×10^{-3}	38.99	
8	1	0.0001	2.94×10^{-8}	394.	14.6	37.04	Fit to 0–400 s of Fig. 4a
8	2	1.000	2.94×10^{-4}	0.0110	4.93×10^{-4}	44.98	
8	3	-0.590	-1.74×10^{-4}	-0.00446	-1.24×10^{-4}	27.93	
8	4	-5.762	-1.70	0.00201	5.40×10^{-5}	26.91	
8	5	0.0001	2.94×10^{-8}	388.	13.6	35.04	
8	6	-1.000	-2.94×10^{-4}	0.0110	3.68×10^{-4}	33.55	
8	7	5762	1.70	0.00201	7.82×10^{-5}	39.01	
8	8	0.590	1.74×10^{-4}	-0.00446	-1.74×10^{-4}	38.99	
10	1	5.183×10^{-5}	1.137×10^{-8}	1.188×10^4	441.	37.04	Fit to 0–400 s of Fig. 4a
10	2	40.01	0.01200	0.04973	2.23×10^{-3}	44.98	
10	3	129.0	0.03900	0.04662	1.30×10^{-3}	27.93	
10	4	-5.442.	-1.662	1.904×10^{-5}	5.14×10^{-7}	26.91	
10	5	-169.0	-0.05200	0.04744	1.54×10^{-3}	32.58	
10	6	5.252×10^{-5}	1.438×10^{-8}	1.120×10^4	420.	35.04	
10	7	-2.010.	-0.6140	0.005668	1.87×10^{-4}	33.03	
10	8	3.496.	1.068	0.002780	9.35×10^{-5}	33.55	
10	9	2.524.	0.7710	0.005402	2.11×10^{-4}	39.01	
10	10	-3.875.	-1.183	0.003065	1.19×10^{-4}	38.99	

indicated. The actual potential established could also be a function of the pH of the acting solution. pH values of 8 to 9 resulted in an aluminum redox potential of -1.66 V^{11} while higher pH values may result in slightly different redox potentials.

A rate of reaction for fluoride ion replacing hydroxide ion has been reported²³ in a pH region of 4 to 5 as $K_1 = 303\text{ mol}^{-2}\text{ s}^{-1}$, $K_2 = 5\text{ mol}^{-1}\text{ s}^{-1}$, and $K_3 = 1.03 \times 10^5\text{ mol}^{-2}\text{ s}^{-1}$. These values are higher than the value of k_2 presented in Table IVB. Reaction rates measured in liquids assume no boundaries (barriers) to diffusion along reaction coordinates so molecular motion proceeds as though in an infinite liquid. Reactions that proceed on a reactive surface, such as this example, are anticipated to be slower since half of the free volume is missing (semi-infinite model), diffusion near a solid surface may be slower and formation of interfacial barriers (and double layers) may further restrict molecular motion. The experimental data indicated this reaction rate to be $\omega_2 = 4.97 \times 10^{-2}/\text{s}$. Higher rates produced in the presence of selected ligands,²³ shown to reversibly displace fluoride ion at pH 9 as a subsequent reaction, also indicated this step may be slow.

The rate of dissolution of $\text{Al}(\text{OH})_3$ has also been measured²⁴ under mildly acidic conditions indicating two distinct, apparently age-dependent, rates. Amorphous $\text{Al}(\text{OH})_3$ yielded a dissolution rate of $k'_a = 0.45/\text{s}$ such that $C(t) = C_0 e^{-0.45t}$ while aged or possibly less hydrated $\text{Al}(\text{OH})_3$ yielded a dissolution rate of $k'_c = 0.0095/\text{s}$ so $C(t) = C_0 e^{-0.0095t}$. These constants are identified as frequency factors in the present discussion so the apparent equivalent second-order rate constants would be $k_a = 3.5 \times 10^{-2}\text{ L/mol s}$ and $k_c = 7.4 \times 10^{-4}\text{ L/mol s}$. Here the rates of dissolution of a suspended solid and that of a hydrated aqueous gel differ by nearly two orders of magnitude. The lower value was still orders of magnitude different from that of a liquid-solid interface anticipated for dissolution of a passivated aluminum surface. The data for Eq. 22 in Table IVB, also of a solid-liquid interface, indicates the reaction rate to be $\omega_4 = 1.90 \times 10^{-5}/\text{s}$ still slower than that of $k'_c = 9.5 \times 10^{-3}/\text{s}$ above. The small value seems reasonable considering dissolution of aluminum occurs only at the solid-liquid interface at a measured rate of $<10\text{ nm/min}$.¹

Constants for Eq. 20 indicate the small reaction rate of $\omega_2 = 4.97 \times 10^{-2}/\text{s}$ to be orders of magnitude higher than for dissolution of surface aluminum metal. Dissolution of aluminum fluoride, Eq. 21 might be anticipated to be similar to ω_2 with a value of $\omega_3 = 4.66 \times 10^{-2}/\text{s}$. The chemical potential for this dissolution was shown to be $\mu'_3 = 3.90 \times 10^{-2}\text{ V}$.

The chemical potential constant derived for the more complex reversible ammonium fluoride reaction in formulation FA, $\mu'_1 = 1.14 \times 10^{-8}\text{ V}$, was similar to the equilibrated or reversible chemical reaction FB of $\mu'_1 = 5.57 \times 10^{-8}\text{ V}$ yet the equilibration rate constant for formulation FA of $\omega_1 = 1.19 \times 10^4/\text{s}$ was nearly two orders of magnitude higher than that for formulation FB of $\omega_1 = 3.96 \times 10^2/\text{s}$, refer to data of Table IIIB. The values of $\mu'_2 = -7.27 \times 10^{-11}\text{ V}$ and $\omega_2 = 3.20 \times 10^{-5}/\text{s}$ for the FB formulation and the values of $\mu'_2 = 1.20 \times 10^{-2}\text{ V}$ and $\omega_2 = 4.97 \times 10^{-2}/\text{s}$ for the FA formulation indicate a shift in the chemical potentials and reaction rates. The values for the dissolution of aluminum also show significant differences between the two different types of chemistry. For formulation FB values of $\mu'_4 = -1.65\text{ V}$ and $\omega_4 = 1.71 \times 10^1/\text{s}$ indicated a substantial value for the rate constant while the rate constant for formulation FA, of $\omega_4 = 1.90 \times 10^{-5}/\text{s}$ was orders of magnitude lower as anticipated for a passivated surface. This result correlates well with dissolution of Al in formula FB and passivation of Al in formula FA.

The very small apparent chemical potentials for chemical equilibrium Eq. 19 and 24 imply some energy, though negligible, is associated with these balances. Nonetheless, non-zero values of chemical potentials must be associated with these chemistries. Application of the time-dependent free energy formalism indicated that

a chemical potential and a reaction rate could be associated with every chemical reaction equation.

Results of these analyses provided a conceptual chemical model for dissolution (corrosion) of aluminum metal similar to that proposed in the previous article,¹ although it has become apparent that variations in the chemical model set for more than eight chemical reaction equations was indicated. This approach to analysis of OCP curves, specifically corrosion of materials as represented by an energy vs. time curve, demonstrated the applicability of the mathematical formalism for simultaneously extracting details of both the thermodynamic process and kinetic reaction rates. While there were difficulties in analysis of convoluted experimental curves representing more than four sets of chemical reactions, the analysis process has been informative.

Conclusions

Development of a mathematical formalism expressing changes in thermodynamic free energy of a chemical system as a function of time, for description of experimental time-dependent energy curves such as the OCP metal corrosion plots, produced results in terms of chemical potentials and reaction rates, one pair of constants for each causal chemical reaction. Experimental OCP data was presented in terms of aluminum surface removal (corrosion) models consisting of sets of four to ten chemical reactions. Furthermore, derived reaction rates and chemical potentials for the known $\text{Fe}(\text{II}) + \text{I}_2$ reaction were found to be in good agreement with known values. The formalism has been helpful in describing results of OCP metal corrosion plots of IC interconnects cleaned by silicon wafer remover products. It has also enabled modified chemistry to be developed (formula FA compared to formula FB) for reduction of the amount of surface material removed (corroded) during the cleaning process.

DuPont Electronics Technologies, EKC Technology, assisted in meeting the publication costs of this article.

References

1. M. K. Carter, R. Small, M. Cernat, and B. Hansen, *J. Electrochem. Soc.*, **150**, B52 (2003).
2. S. W. Benson, *The Foundations of Chemical Kinetics*, Chap. III, McGraw-Hill Book Co., Inc., New York (1960).
3. G. N. Lewis, M. Randal, K. S. Pitzer, and L. Brewer, *Thermodynamics*, 2nd ed., p. 75, McGraw-Hill Book Co., Inc., New York (1961).
4. S. W. Benson, *The Foundations of Chemical Kinetics*, p. 17, McGraw-Hill Book Co., Inc., New York (1960).
5. S. W. Benson, *The Foundations of Chemical Kinetics*, pp. 73-75, McGraw-Hill Book Co., Inc., New York (1960).
6. A. J. Bard and L. R. Faulkner, *Electrochemical Methods*, pp. 58-62, John Wiley & Sons, New York (1980).
7. J. O'M. Bockris and S. U. M. Khan, *Surface Electrochemistry*, pp. 75-83, Plenum Press, New York (1993).
8. C. Kittel, *Introduction to Solid State Physics*, 2nd ed., p. 279, John Wiley & Sons, Inc., New York (1961).
9. G. B. Arfken and H. J. Weber, *Mathematical Methods for Physicists*, p. 669, Harcourt Academic Press, New York (2001).
10. G. B. Arfken and H. J. Weber, *Mathematical Methods for Physicists*, p. 401, Harcourt Academic Press, New York (2001).
11. C. J. Marek, *Technical Support Package, Physical Sciences*, (no. 176), Lewis Research Center, Cleveland, OH, www.nasatech.com/Briefs/Jan (1998).
12. *CRC Handbook of Chemistry and Physics*, D. R. Lide, Editor-in-Chief, 81st ed., Appendix A, Mathematical Tables, pp. A2-A6, CRC Press, New York (2000-2001).
13. *CRC Handbook of Chemistry and Physics*, D. R. Lide, Editor-in-Chief, New York, 81st ed., 8-21, Petr Vanysek, Section Editor, CRC Press, New York (2000-2001).
14. D. Kivelson and H. Friedman, *J. Phys. Chem.*, **93**, 7026 (1989).
15. A. Neudeck and J. Ditttrich, *J. Electroanal. Chem.*, **313**, 37 (1991).
16. L. Kekedy, M. Olariu, and F. Kormos, *Analisis*, **10**(6), 288 (1982).
17. D. Nordstrom, *Geochim. Cosmochim. Acta*, **41**, 1835 (1977).
18. D. Tench and E. Yeager, *J. Electrochem. Soc.*, **121**, 318 (1974).
19. V. Gutmann, G. Gritzner, and K. Danksagmuller, *Inorg. Chim. Acta*, **17**, 81 (1976).
20. C. Larrogue, P. Maurel, and P. Douzou, *Biochim. Biophys. Acta*, **501**, 20 (1978).
21. H. Kaneko, T. Aoki, A. Negishi, and K. Nozaki, in *Proceedings of the 41st Meeting of the ISE*, Prague, TU 178 (1990).
22. P. Neta, R. E. Huie, and A. B. Ross, *J. Phys. Chem. Ref. Data*, **17**, 1208 (1988).
23. K. Srinivasan and G. A. Rechnitz, *Anal. Chem.*, **40**, 1818 (1968).
24. E. Lydersen, B. Salbu, A. B. S. Poleo, and I. P. Muniz, *Water Resour. Res.*, **27**, 351 (1991).